10th International Conference on Fracture Mechanics of Concrete and Concrete Structures
FraMCoS-X
G. Pijaudier-Cabot, P. Grassl and C. La Borderie (Eds)
https://doi.org/10.21012/FC10.233198

ANALYSIS OF FIBER-MATRIX INTERACTION IN FRC USING X-RAY TOMOGRAPHY AND DIGITAL VOLUME CORRELATION

M. FLANSBJER[*], N. WILLIAMS PORTAL[*], S. HALL[†] AND J. ENGQVIST[†]

[*] RISE Research Institutes of Sweden
501 15 Borås, Sweden
e-mail: mathias.flansbjer@ri.se, natalie.williamsportal@ri.se, www.ri.se

†Lund University
221 00 Lund, Sweden
e-mail: stephen.hall@solid.lth.se, jonas.engqvist@solid.lth.se, www.lth.se

Key words: Fiber Reinforced Concrete, Pull-Out Behavior, X-ray Computed Tomography, Digital Volume Correlation

Abstract: Fiber pull-out is generally considered to be the dominating failure mechanism in fiber reinforced concrete (FRC). Accordingly, pull-out tests are typically performed to characterize the fiber-matrix interaction. However, little direct insight can be gained on the actual mechanisms of the pull-out from such a test. Deeper understanding could however be gained through the addition of non-destructive techniques to pull-out tests to enable the visualization and quantification of the mechanical interaction. Pull-out mechanisms for different common steel fibers were investigated using adapted pull-out tests performed in-situ in an X-ray micro tomography (µXRT). High-resolution volume images from the µXRT scans enable clear visualization of aggregates, pores, fiber and fiber-matrix interface. Furthermore, the natural density speckle pattern from aggregate distribution and pores was found to be suitable for Digital Volume Correlation (DVC) analysis. From the DVC results it was possible to visualize and quantify the strain distribution in the matrix around the fiber at different load levels up to final failure, being marked by either pull-out or fiber rupture. The load transfer mechanism was initially dominated by shear along the fiber. As the load increased, slip occurred in the end-hook region and mechanical locking became the governing mechanism. This study demonstrates that strain measurements within the concrete matrix and passive end-slip can be obtained successfully using µXRT imaging and DVC analysis, which leads to an increased understanding of the interaction mechanisms in fiber reinforced concrete under mechanical loading.

1 INTRODUCTION

The main benefit of fibers is their ability to bridge cracks and thereby improve the fracture characteristics of concrete. Fiber pull-out is generally considered to be the dominating failure mechanism in fiber reinforced concrete (FRC) to mitigate brittle failure. Provided that fiber rupture is avoided, debonding between fiber and concrete starts on the shortest embedded lengths until full debonding occurs and the fiber is gradually pulled-out. Accordingly, pull-out tests are typically performed on FRC to characterize the fiber-matrix behavior. However, little direct insight can be gained on the actual mechanisms of the pull-out from such tests, whereas, a deeper understanding of the underlying interaction mechanisms between discrete fibers and the surrounding concrete matrix could clearly lead to optimized FRC. Such deeper understanding could be gained through the addition of non-destructive techniques to pull-out tests to enable the visualization and quantification of the mechanical interaction between the fibers and the concrete matrix.

X-ray micro-tomography (μXRT) is a non-destructive 3D imaging technique that has in recent years become a useful tool in engineering and material science to characterize the internal structures and mechanisms of a wide range of materials [1,2]. μXRT has most commonly been applied on unloaded material samples, but with in-situ devices it is possible to run mechanical tests within a tomograph thus enabling scanning during loading of specimens [3]. Coupling of μXRT with Digital Volume Correlation (DVC) has been applied to analyze the interior structural evolution of an array of materials, e.g., concrete [4], bone [5], wood [6], rock [7] and granular materials [8]. DVC can essentially be considered as an extension of Digital Image Correlation (DIC) applied to tomographic image volumes to calculate full 3D vector displacements, from which tensor strain fields can be derived.

This paper presents the development of a method enabling the visualization and quantitative analysis of the fiber-matrix interaction on a meso-mechanical level in FRC samples. Reference tests are firstly described that provided characterization of the pull-out behavior of a steel fiber centrically cast in small cylindrical concrete specimens. These tests were also used to determine load levels at which μXRT imaging was performed during pull-out tests in-situ in an X-ray tomograph. The pull-out test rig, tailored to the constraints of the μXRT equipment and mechanical loading configuration, is described herein. Results from the tests and analysis, including using DVC, are presented and discussed for one fiber type in terms of the mechanical processes occurring in and around the fiber.

2 MATERIALS AND METHODS

2.1 Selected Materials and Test Specimens

Cylindrical concrete specimens with a height of 50 mm and a diameter of 43 mm, each containing a singular steel fiber partly cast-in, perpendicular and centric to the concrete surface (Figure 1a) were specifically designed to accommodate a test setup having the possibility to apply a pull-out load while being placed in a tomograph. The embedded length, L_e, was set to 30 mm for all specimens.

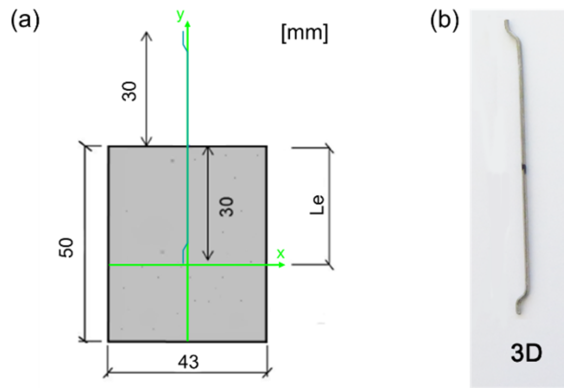

Figure 1: (a) Specimen geometry and (b) photo of Dramix 3D fiber.

In total, six different steel fiber alternatives were selected for investigation. These fibers have varying anchorage characteristics such as hooked-ends, hooked and flattened ends and wavy structure. However, the scope of this paper is limited to the investigation of Dramix 3D 65/60 from Bekaert, as illustrated in Figure 1b. This fiber has a nominal length of 60 mm, a diameter of 0.9 mm and a tensile strength of 1000 MPa.

A fine-grained high-performance concrete mix developed for use in fiber-based reinforced concrete composites was used. This concrete mixture includes a CEM II/A-V 52.5 N Portland-fly ash cement, additional fly ash, chemical admixtures and a maximum aggregate size of 4 mm. The concrete was measured to have a compressive strength of 70 MPa and a tensile strength of 3.2 MPa at the age of 28 days.

2.2 Reference Pull-Out Tests

A single-sided pull-out test was adopted within the project, based on knowledge gathered from other studies (e.g., [9]). This method makes it possible to characterize the behavior of individual fibers when pulled-out of the concrete matrix in terms of a load versus displacement relationship. Pull-out tests were firstly conducted without µXRT according to Figure 2 to characterize the load-displacement relationship for the different FRC specimens.

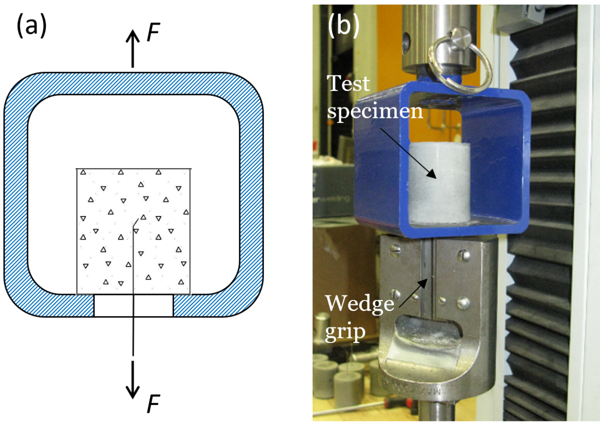

Figure 2: (a) Illustration and (b) photo of reference pull-out test set-up.

The specimen was supported around its outer edge by a steel fixture and the free end of the fiber was clamped in a wedge grip. The loading was controlled at a constant displacement rate of 0.1 mm/min. Based on the outcome of the results of these tests, the final test schedule and load levels for the pull-out tests with µXRT were established.

2.3 Pull-Out Tests with µXRT

The in-situ pull-out tests were performed in the Zeiss XRM520 at the 4D Imaging Lab at Lund University. A test specimen affixed to the loading device and a schematic of the test set-up are shown in Figure 3. Each specimen was mounted on the top of the device and supported around its outer edge by a PMMA tube. The fiber protruding from the specimen was glued with HBM X60 into a threaded end anchorage that was screwed onto the piston of the test rig. The pull-out load was applied by controlled displacement of the piston.

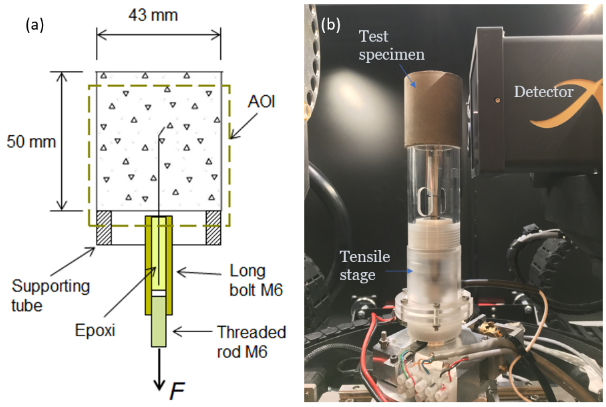

Figure 3: (a) Illustration of pull-out test setup up (cross section) and (b) overview of the µXRT test set-up.

The µXRT acquisitions involved 1601 radiographic projections over 360° with a 2 s exposure time using a source voltage of 160 kV and power of 10 W plus the He3-filter (as provided by the manufacturer) to reduce beam hardening artefacts. A 0.4× objective was used, and the camera binning was set to 2 × 2 giving images of 1024 × 1024 px. The voxels in the final reconstructed volumes were cubic with side lengths of 55 µm.

For each in-situ test, an initial scan was taken of the specimen prior to loading, which provided the undeformed reference image for the subsequent DVC-analyses. Thereafter, each specimen was loaded stepwise to the prescribed load levels at which new scans were made. One complete scan of the specimen took about 1 h at each load level, which amounts to approximately one working day to execute a full test.

2.4 Processing with DVC

The StrainMaster software from LaVision was used for the DVC analyses. The imported volume image is discretized into smaller sub-volumes containing a unique grey-scale pattern. The software then correlates the pattern from the reference image to the deformed images and calculates the displacement within each sub-volume. This results in a full 3D vector field representing the specimen displacement, from which tensor strain fields are derived.

In this study, the volume image of the specimen was reduced to a smaller sub-region around the fiber before it was imported to the DVC code, see Figure 4. The sub-volume size was set to 24 × 24 × 24 voxels and the sub-volume overlap to 75%. This is approximately equivalent to a sub-volume size of 1.3 × 1.3 × 1.3 mm and a resultant grid resolution of 0.3 × 0.3 × 0.3 mm.

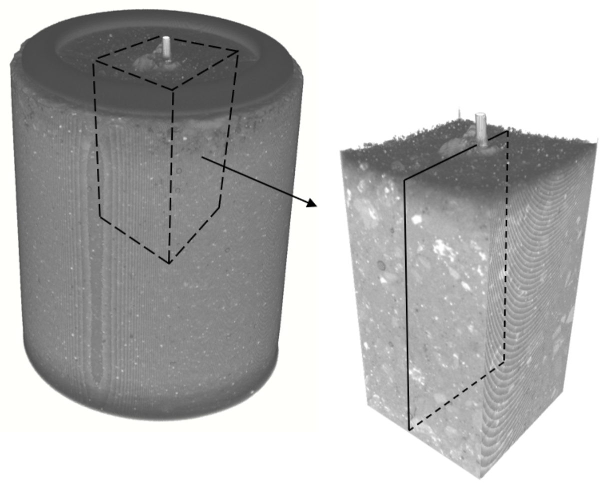

Figure 4:Volume image of the entire pull-out specimen and the reduced sub-region for DVC.

The region outside the specimen and the steel fiber itself was excluded from the DVC analysis using an algorithmic masking. It is to say that lower and upper threshold limits of the grey-scales in the volume image were specified. Furthermore, for a sub volume to be used, the requirement of minimum number of valid voxels inside the sub volume was set to 90%. This provides more reliable results at the edge of the analyzed volume and, most importantly in this case, at the fiber-matrix interface.

3 RESULTS AND DISCUSSION

3.1 Fiber-matrix pull-out behavior

Reference tests to determine the fiber-matrix pull-out behavior were performed on three specimens with Dramix 3D fibers, denoted as 3D-1, 3D-2 and 3D-3 (Figure 5). Pull-out failure was obtained in one test, while fiber rupture was obtained inside the specimen in two of the tests.

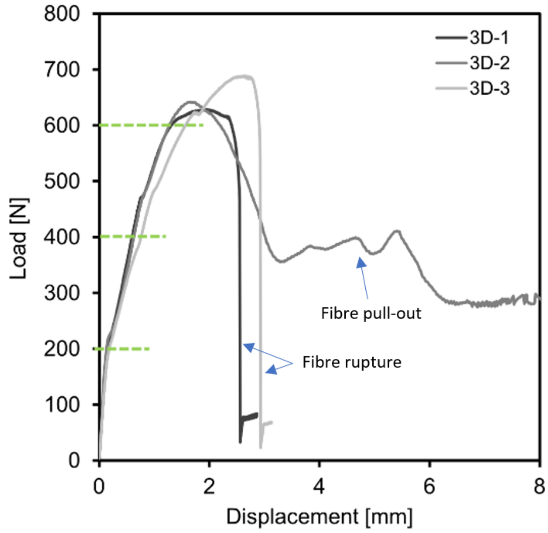

Figure 5: Pull-out load vs displacement for 3D specimens with indicated load levels for µXRT.

Suitable load levels for the pull-out tests with µXRT are indicated on the load-displacement curves. Load levels prior to the peak load are relevant to be able to capture the initial debonding of the fiber and transition from mechanical adhesion to frictional bond. At load levels approaching the peak load, it is hypothesized that plastic deformation of the fiber can likely be expected. In the case of pull-out failure, it could also be relevant to capture the extent of plastic deformation and pull-out of the fiber within the post-peak region.

3.2 Fiber-matrix interaction

Two specimens with Dramix 3D fibers were tested in-situ in the µXRT, denoted as 3D-4 and 3D-5. Each specimen was imaged by µXRT at different load levels selected based on the load-displacement relations obtained in the reference pull-out tests. Images were acquired before and after peak load, as depicted in Figure 6. Since the displacement was kept constant during the time of scanning, some relaxation in load could be observed at some of the scanning occasions. The response of specimen 3D-5 was characterized by a typical fiber pull-out behavior with a maximum load of 610 N, while the failure mode for 3D-4 was marked by fiber rupture at a slightly higher maximum load of 670 N.

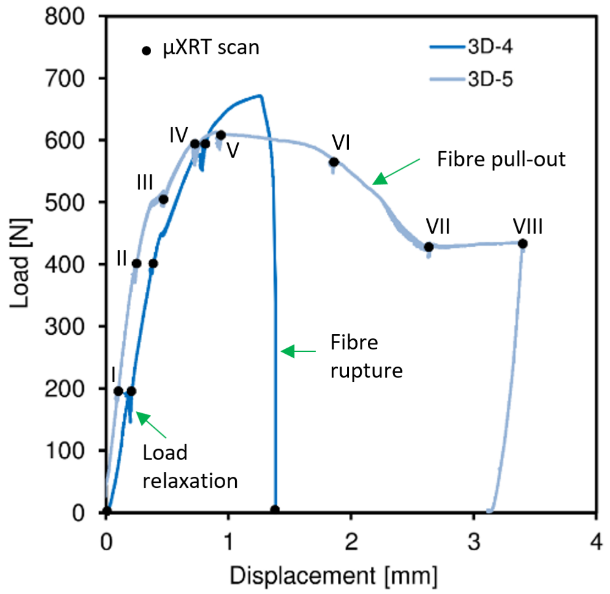

Figure 6: Pull-out load vs displacement for 3D-4 and 3D-5 with indicated load levels for µXRT scanning.

From the volume reconstruction of the high-resolution µXRT images, it was possible to have clear visualization of aggregates, pores and the fiber. The volume images provide a great deal of information related to both the geometry of the test specimen and the internal mechanisms taking place during loading. It is possible to distinguish the fibers final position in the specimen as well as the aggregate and pore distribution at the fiber interface. Moreover, the slipping or rupturing of the fiber within the so-called fiber canal can also be visualized.

Figure 7 presents how the hooked steel fiber in specimen 3D-5 deformed and slipped inside the canal at four different stages of the loading. The passive end-slip was evaluated as the distance between the fiber end and the bottom of the fiber canal. The first fiber end slip was observed at the 600 N load level in both tests; with a slip value of 0.09 and 0.15 mm for 3D-4 and 3D-5, respectively. The slip initiation is likely related to the change in load-displacement curve (Figure 6) that can be observed at approximately 450 N for 3D-4 and 500 N for 3D-5. The test of specimen 3D-4 ended with a fiber rupture, while a continuous fiber pull-out was observed for specimen 3D-5 in the following load stages during the post-peak region (Figure 8).

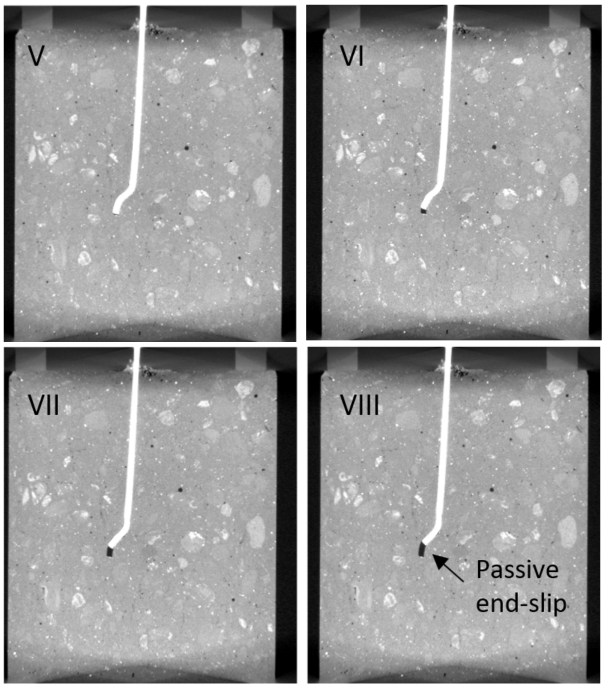

Figure 7: µXRT images at selected load levels for specimen 3D-5. The numbers refer to load stages in Figure 6.

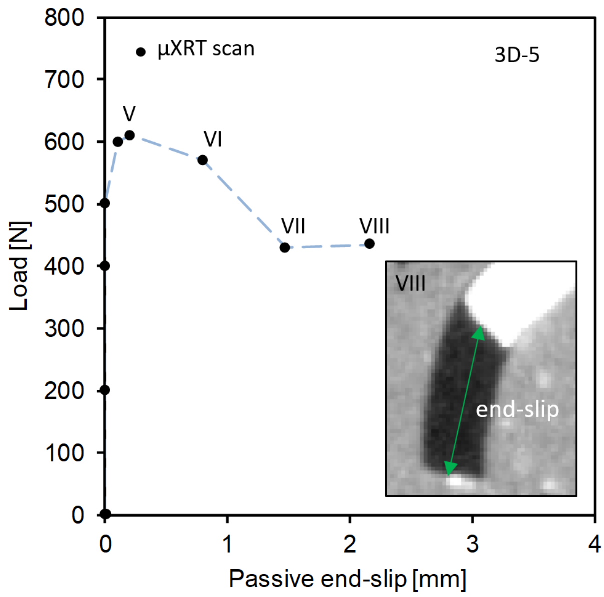

Figure 8: Pull-out load vs passive end-slip for 3D-5. The numbers refer to the images in Figure 7.

Figure 9 shows the deformed fiber in specimen 3D-5 at different load stages in relation to its original position. In addition, Figure 9 (right) presents the deformed shape of the same fiber at the last µXRT scanning (point VIII), with two highlighted regions at the hook showing noticeable fiber necking.

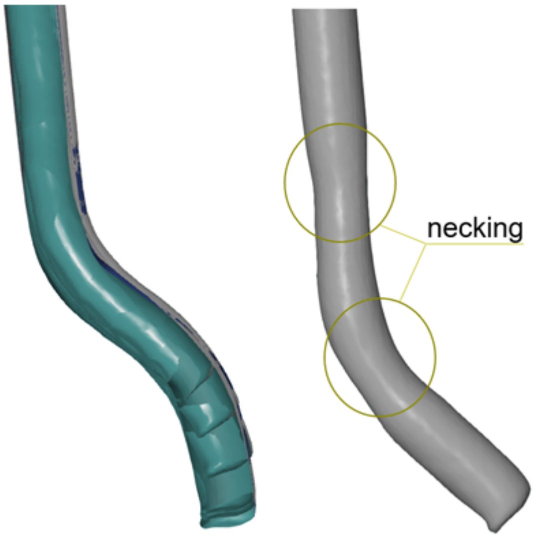

Figure 9: Visualization of successive fiber deformation and end-slip (stage IV-VIII), and fiber necking at the hook for 3D-5 (stage VIII).

The natural grey-scale speckle in the volume images due to the aggregate distribution and pores was found to be suitable for DVC analysis. The DVC analysis of the time-series of images enabled the quantification of strains in the sample as well as the visualization of process details that were not visible simply from the tomography images. Most importantly, it is possible to observe the change in load transfer mechanism between the steel fiber and the concrete matrix during the pull-out loading, going from bond along the fiber to mechanical locking at the end-hook.

During the initial linear part of the load-displacement curve, elevated shear strains can be observed along and around the fiber, which according to theory can be due to adhesion and frictional bond, as shown in Figure 10. At the first load level of 200 N, higher shear strains are mainly located at the upper part where the fiber protrudes from the specimen, for both 3D-4 and 3D-5. The latter also exhibits some localized regions with higher shear strains further down along the fiber. At the next load level of 400 N, higher shear strains developed along the fiber and towards the fiber end.

Hence, it is possible to follow the advancement of the debonded zone along the fiber-matrix interface with increasing pull-out load. However, in future studies it is suggested to perform tests on cylindrical specimens with a reduced diameter to obtain increased volume image resolution and, thereby, be able to better resolve the strain fields in the close vicinity of the fiber-matrix interface in the DVC analysis. Furthermore, to follow the interface debonding process more closely, µXRT imaging is suggested to be performed at more closely spaced load levels during the initial pre-peak part of pull-out response.

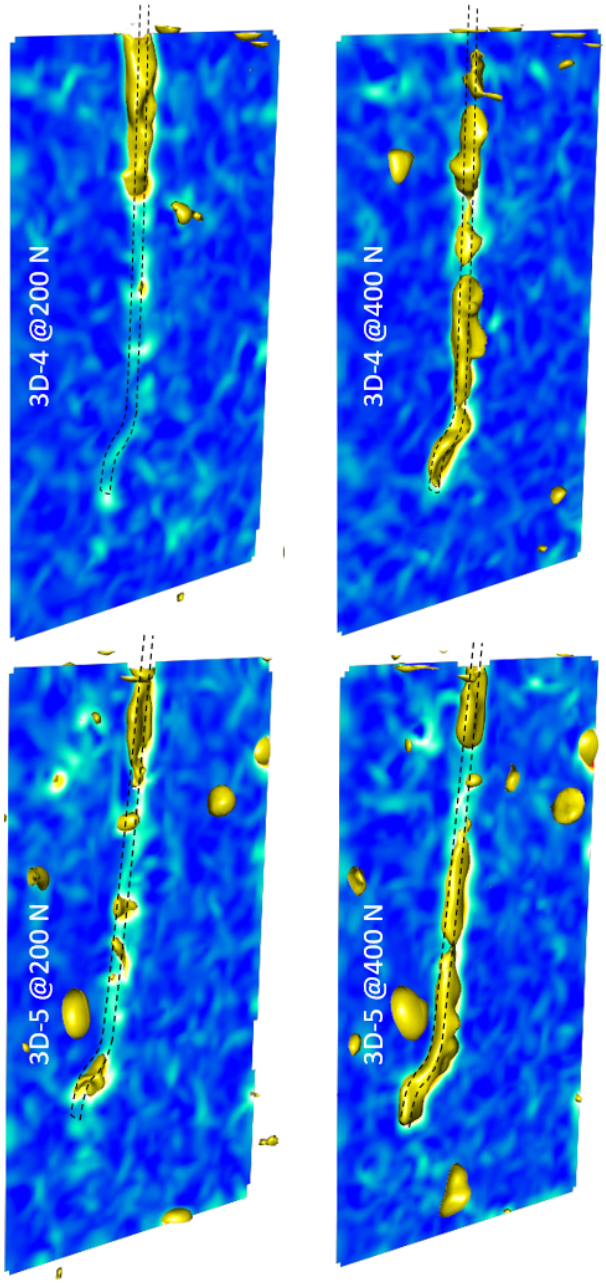

Figure 10: Shear strain along the fiber in 3D-4 and 3D-5, at a load level of 200 and 400 N (Stages I and II). Yellow 3D ISO-surface indicate 2% shear strain. The location of the fiber is indicated by a dashed line.

When debonding reaches the end-hook, the hook acts as a mechanical interlock since the fiber is forced to deform to be able to slip. The load transfer between the fiber and matrix becomes thereby localized at the hook, resulting in high compressive strains (minimum principal strains) due to local crushing of the matrix (Figure 11).

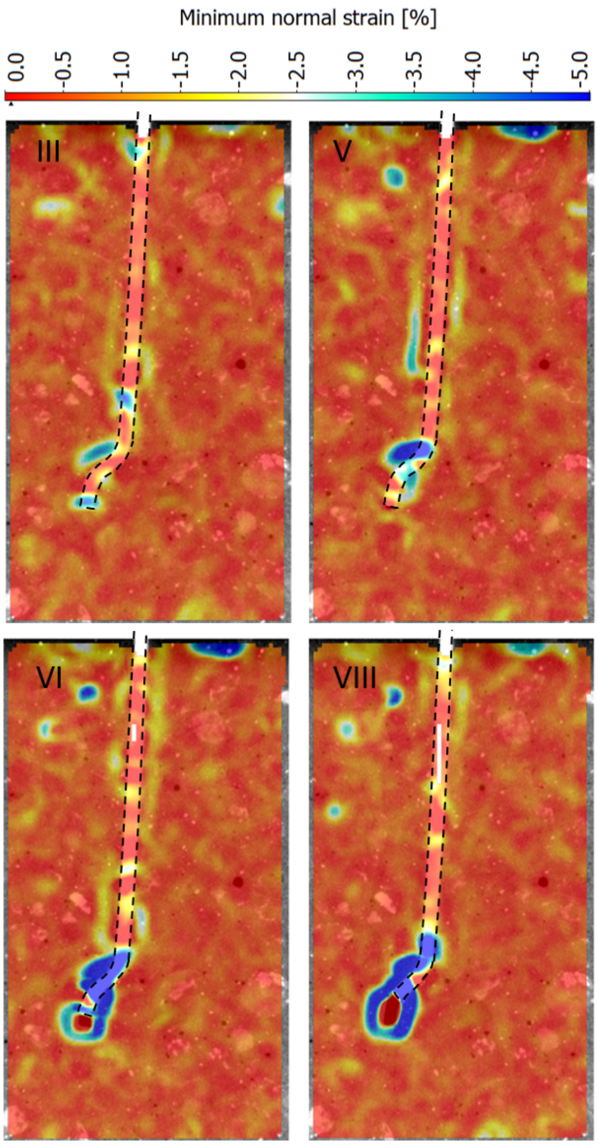

Figure 11: Minimum principal strain at the end-hook in 3D-5 at selected load stages (see Figure 6).

The size of the compressed region around the fiber increases as well as the magnitude of the compressive strain during loading. The development of maximum compressive strain at the hook region is presented for 3D-4 and 3D-5 in Figure 12. There is a good correspondence in strain development between the specimens in the initial stages, while it starts to differ more closer to peak load, likely due to the different failure modes experienced.

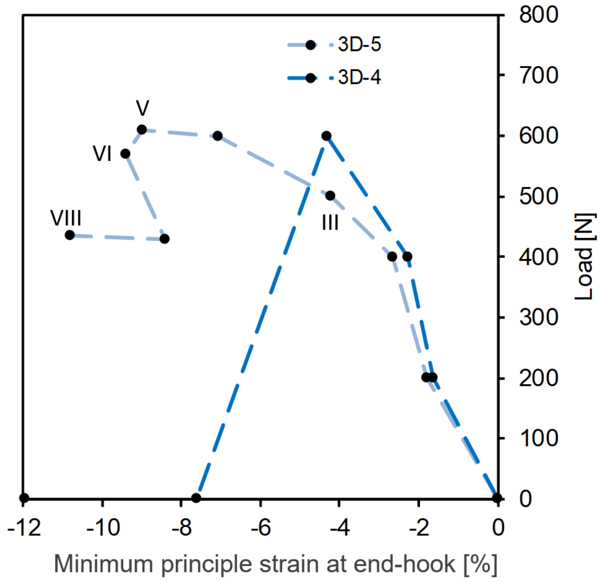

Figure 12: Development of minimum principal strain at the fiber hook for 3D-4 and 3D-5. The numbers refer to the images in Figure 11.

From the results it can be concluded that mechanical locking is still active also for larger end slip values within the post-peak regime of 3D-5. This mechanical locking effect is presumed to be active until the fiber hook has deformed plastically, straightened out and slipped into the main straight canal. The strains that are surrounding the bottom of the fiber canal are thought to be caused by the contraction of the void left by the fiber.

4 CONCLUSIONS

Pull-out mechanisms for steel fibers were investigated using adapted pull-out tests performed in-situ in a µXRT. High-resolution volume images from the µXRT scans enable clear visualization of aggregates, pores, the fiber and the fiber-matrix interface. Furthermore, the natural density speckle pattern from aggregate distribution and pores was found suitable for DVC analysis. From the DVC analysis, it was possible to visualize and quantify the strain distribution in the matrix around the fiber at the different load levels up to final failure, which was marked by either pull-out or fiber rupture. The load transfer mechanism was initially dominated by shear along the fiber. As the load increased, slip occurred in the end-hook region and mechanical locking became the governing mechanism. This study demonstrates that strain measurements within the concrete matrix and at a fiber interface can be obtained successfully using μXRT imaging and DVC analysis, which leads to an increased understanding of the interaction mechanisms between the fiber and the concrete matrix.

REFERENCES

[1] Maire, E. and Withers, P.J., 2014. Quantitative X-ray tomography. *Inter. Mater. Rev., 59*, 1–43.

[2] Landis, E.N., Keane, D.T., 2010. X-ray microtomography. *Mater. Char.,* 61, 1305–1316.

[3] Buffiere, J.Y., Maire, E., Adrien, J., Masse, J.P. and Boller, E., 2010. In Situ Experiments with X-ray Tomography: An Attractive Tool for Experimental Mechanics. *Exp. Mech.*, 50, 289–305.

[4] Yang, Z.J., Ren, W.Y., Mostafavi, M.A., Mcdonald, S.A. and Marrow, T.J., 2013. Characterisation of 3D fracture evolution in concrete using in-situ X-ray computed tomography testing and digital volume correlation. Proc. of the VIII Inter. Conf. on Fract. Mech. of Conc. and Conc. Struct., Toledo, Spain, 10–14 March 2013.

[5] Gillard, F., Boardman, R., Mavrogordato, M., Hollis, D., Sinclair, I., Pierron, F. and Browne, M., 2014. The application of digital volume correlation (DVC) to study the microstructural behaviour of trabecular bone during compression. *J. Mech. Behav. Biomed. Mater.*, 29, 480–499.

[6] Forsberg, F., Sjödahl, M., Mooser, R., Hack, E. and Wyss, P., 2010. Full Three-Dimensional Strain Measurements on Wood Exposed to Three-Point Bending: Analysis by Use of Digital Volume Correlation Applied to Synchrotron Radiation Micro-Computed Tomography Image Data. *Strain*, 46, 47–60.

[7] Mao, L., Zuo, J., Yuan, Z. and Chiang, F.P., 2015. Full-field mapping of internal strain distribution in red sandstone specimen under compression using digital volumetric speckle photography and X-ray computed tomography. *J. Rock Mech. Geotech. Eng.*, 7, 136–146.

[8] Hall, S.A., Bornert, M., Desrues, J., Pannier, Y., Lenoir, N., Viggiani, G. and Bésuelle, P., 2010. Discrete and continuum analysis of localised deformation in sand using X-ray μCT and volumetric digital image correlation. *Géotechnique*, 60, 315–322.

[9] Breitenbücher, R., Meschke, G., Song, F. and Zhan, Y., 2014. Experimental, analytical and numerical analysis of the pullout behaviour of steel fibres considering different fibre types, inclinations and concrete strengths. *Struct. Concr.*, 15, 126–135.